FINAL REPORT

for

NASA Grant NSG 5301

RESEARCH IN ATMOSPHERIC CHEMISTRY AND TRANSPORT

Yuk L. Yung

Principal Investigator

Division of Geological and Planetary Sciences

California Institute of Technology

Pasadena, California 91125

Grant Period

September 15, 1978 to January 14, 1982

NASA Technical Officer
Dr. J.E. Hansen
Goddard Institute for Space Studies
2880 Broadway
New York, New York 10025

Carbon monoxide is the third (after carbon dioxide and methane) most abundant carbon species in the atmosphere, but its current roles in the atmospheric and biogeochemical cycle of carbon are not quantitatively understood. Early work on carbon monoxide included its discovery in the infrared solar absorption spectrum by Migeotte (1948) and an investigation its potential sources and sinks by Bates and Witherspoon (1952). The subject remained dormant for nearly two decades until the importance of the hydroxyl radical in tropospheric chemistry was recognized (Levy, 1971; McConnell et al., 1971). The hydroxyl radical is derived from

$$O_3 + h\nu \rightarrow O_2 + O(^1D) \qquad (R1)$$

$$O(^1D) + H_2O \rightarrow 2OH \qquad (R7)$$

the reaction

$$CO + OH \rightarrow CO_2 + H \qquad (R18)$$

provides the only important sink for CO in the gas phase, and is responsible for determining the chemical lifetime of atmospheric CO. In addition to destroying CO, the hydroxyl radical also destroys CH_4

$$CH_4 + OH \rightarrow H_2O + CH_3 \quad . \qquad (R16)$$

Reaction R16 initiates a sequence of reactions that ultimately lead to the production of CO. As first pointed out by McConnell et al. (1971), R16 represents a major source of CO, especially in the clean troposphere. It was argued (see Wofsy, 1976) that this source, together with that derived from incomplete combination of fossil fuels (Bates and Witherspoon, 1952), could account for the budget of atmospheric CO. However, Biermann et al. (1978) showed that reaction R18, which is primarily responsible for removing CO, is pressure-dependent in the presence of oxygen, and should proceed nearly twice as fast as previously thought. A renewed search for sources of CO suggested that oxidation of non-methane hydrocarbons (NMHC), especially isoprenes and terpenes, emitted by trees (Zimmerman et al., 1978) and biomass burning (Crutzen et al., 1979) could be important. However, it is difficult to quantify the magnitudes of these sources (see Logan et al., 1981 for a detailed catalog and assessment of the uncertainties).

The intense interest and effort on CO in the last decade results in the generation of an extensive data base concerning its spatial distribution (see for example, Seiler, 1974) and seasonal variation (Dianov-Klokov et al., 1978). Previous studies of the CO cycle include photochemical models which neglected horizontal transport (Wofsy, 1976; Crutzen and Fishman, 1977; Logan et al., 1981), and Hameed and Stewart's (1979) model, which considered north-south mixing by diffusion. However, the chemical lifetime of CO is believed to be at least several weeks, and hence both chemistry and transport should play a role in determining the CO concentration as a function of height, latitude and season. A study of the CO cycle with a three-dimensional global model, which explicitly accounts for atmospheric motions, should therefore be useful for helping to identify and quantify the sources and sinks of CO. The exercise is meaningful because an important part of our knowledge of CO is fairly well constrained: we can calculate the OH concentration in the troposphere to within a factor of 2 (OH determines the lifetime and methane oxidation source of CO), and we can estimate the anthropogenic (industrial) source with similar accuracy. The existing data sets offer roughly three independent pieces of information on CO: (a) latitudinal variation, (b) vertical variation, especially in the tropical upper troposphere and (c)

seasonal variation at mid-latitude. In our model, there is essentially only one free parameter, the magnitude of the plant (NMHC) source in the tropics. A large number of other parameters have also been tested, but they were shown to be unimportant. The concentrations of the hydroxyl radical are computed self-consistently. Since the lifetime of CO strongly affects its spatial and temporal variations, we consider our derived OH concentration as empirical values that satisfy the CO observations, and their validity should transcend the assumptions of our simplified chemical model.

In the following report, the essential results of our general circulation model study of CO are presented.

A GENERAL CIRCULATION MODEL STUDY OF ATMOSPHERIC CARBON MONOXIDE

Joseph P. Pinto, Yuk L. Yung*, David Rind, Gary L. Russell,
Jean A. Lerner, James E. Hansen and Sultan Hameed+

Goddard Space Flight Center
Institute for Space Studies
New York, New York 10025

Abstract

The carbon monoxide cycle is studied by incorporating the known CO sources and sinks in a tracer model which uses the winds generated by a general circulation model. The photochemical production and loss terms, which depend on OH radical concentrations, are calculated in an interactive fashion. Comparison of the computed global distribution and seasonal variations of CO with observations is used to yield constraints on the distribution and magnitude of the sources and sinks of CO, and the abundance of OH radicals in the troposphere. We present evidence that there is a substantial low latitude plant source of about 1.3×10^{15} g yr^{-1}, in addition to the anthropogenic and CH_4 oxidation sources. Our results suggest a globally averaged tropospheric OH concentration equal to 7×10^5 cm^{-3}, and that this value might have been 20 percent higher in the pre-industrial atmosphere.

Introduction

Carbon monoxide ~~is a trace component of~~ the atmosphere; whose mixing ratio is in the range $0.5 - 2.5 \times 10^{-7}$ by volume (Migeotte, 1948; Seiler, 1974). The abundance and global distribution of the gas reflects interactions between photochemistry, transport and surface sources and sinks. Quantitative knowledge of the CO cycle is important in its own right, for the information it implies with regard to the global dispersal of atmospheric pollutants, and for an assessment of perturbations of the troposphere by man's activities.

The identity and magnitudes of the major sources and sinks of CO are still uncertain. Suggestions for sources include the incomplete combustion of fossil fuels (Bates & Witherspoon, 1952), the oxidation of methane (McConnell et al., 1971), the oxidation of non-methane hydrocarbons (NMHC) emitted by forests (Zimmerman et al., 1978), marine biological activity (Seiler and Schmidt, 1975) and biomass burning (Crutzen et al., 1979). The primary loss mechanism for CO involves the reaction (see Table 1a)

$$CO + OH \rightarrow CO_2 + H \qquad \text{(R18)}$$

where the hydroxyl radical, OH, is derived from

---

*California Institute of Technology, Pasadena, Ca. 91125
+State University of New York, Stony Brook, New York 11794

$$O_3 + h\nu \rightarrow O_2 + O(^1D) \quad (R1)$$

$$O(^1D) + H_2O \rightarrow 2OH \quad (R7)$$

(Levy, 1971). Uptake by soil micro-organisms (Liebl and Seiler, 1976) may represent an additional minor sink.

Recent estimates of the mean tropospheric OH abundance vary from 1.5 x 10^6 cm^{-3} (Wofsy, 1976) to 2 x 10^5 cm^{-3} (Singh, 1977). Improved estimates of the OH concentration are needed to permit assessment of the impact of anthropogenic releases of halocarbons, such as CH_3CCl_3 and CH_3Br, on stratospheric O_3, as well as for estimating the lifetime of tropospheric pollutants, such as SO_2 and nitrogen oxides (Yung et al., 1975; Sze, 1977; Hameed et al., 1979).

Previous studies of the CO budget and OH include photochemical models which neglected horizontal transport (Wofsy, 1976; Crutzen and Fishman, 1977; Logan et al., 1981), and Hameed and Stewart's (1979) model, which considered north-south mixing by diffusion. However, the chemical lifetime of CO is believed to be at least several weeks, and hence both chemistry and transport should play a role in determining the CO concentration as a function of height, latitude and season. A study of the CO cycle with a three-dimensional global model, which explicitly accounts for atmospheric motions, should therefore be valuable for helping to identify sources and sinks of CO and the concentration of OH.

In the following section we briefly describe the three-dimensional transport model used in our studies. In the subsequent section we describe several experiments used to investigate the CO cycle. In the final two sections we discuss the results and implications of the experiments.

Description of the Model

The numerical experiments of the carbon monoxide cycle were performed with a general circulation model (Hansen et al., 1981). The general circulation model is global in extent, with a horizontal resolution of 8° x 10° (latitude x longitude). Seven layers, evenly spaced in σ co-ordinates, were employed between the surface and 10 mb, (31 km), with at least one layer entirely within the stratosphere at all locations. The model was run for five years, and the necessary dynamical variables for the fifth year stored off line for use in a "tracer model". Compared with climatological data, the three-dimensional wind fields, temperatures, and humidity, are all realistic. An indication of the representativeness of the model's wind fields is presented in Fig. 1a for the surface winds in February and in Fig. 1b for the jet stream winds. The surface wind pattern shows the expected latitudinal variation, with easterlies at low latitudes, and cyclonic and anticyclonic circulations at high latitudes. The southeast and northeast trade winds converge near the equator, the pattern being more apparent over the ocean, where frictional effects are less than over land. Anticyclonic patterns dominate over the oceans near 30° latitude, representative of the subtropic high pressure system. At about 50°N latitude the Aleutian low in the mid-Pacific and the Icelandic low in the North Atlantic produce cyclonic wind patterns, while prevailing westerlies occur over the United States and Asia. In the southern hemisphere strong west winds are evident near 60°S. All these features predicted by our model are in accord with observations. At the jet stream level, strong winds are evident from 30° to 60°N, associated

with the subtropical and the polar jets. Essential features include the enhanced wind velocities near Japan and the east coast of the United States, and a strong poleward component over the far North Atlantic. At low latitudes the jet stream is weak and predominantly easterly. Again, all such model predictions are consistent with observations. For purposes of this work, however, the most relevant dynamical quantities are the meridional transport of water vapor, heat, momentum and angular momentum. A detailed comparison of the values of the above quantities predicted by our GCM and the observations suggest that the agreement is better than 75%. This provides strong evidence that the GCM can simulate the transport of trace species to an accuracy of 75%, adequate for the present investigation. At hourly time steps the instantaneous mass distribution and the averaged horizontal mass fluxes are fed into the tracer program. These mass fluxes are averaged over six hour intervals (Mahlman and Moxim, 1978). The vertical mass fluxes are derived from the horizontal mass fluxes and the continuity equation. We also included monthly-averaged vertical mixing by dry and moist convection. Advection of a tracer is accomplished by a novel finite differencing technique. For each grid box we predict four prognostic quantities: the mean concentration of the tracer n, and its spatial gradient ∇n. The scheme determines the four quantities for the next time step using an upstream method. This algorithm is comparable in accuracy to a fourth order scheme (Mahlman and Sinclair, 1977), but it has much less numerical noise. The mathematical details are presented in Russell and Lerner (1981).

The chemical sources and sinks of CO in the tracer continuity equation are provided by a simplified chemical model, which is described in greater detail below. The concentration of the OH radical at each grid point is calculated using the current abundance of CO. We then use this value of OH to calculate the methane oxidation source (R16) as well as the chemical sink (R18) for CO. The values of OH are updated monthly, which is sufficiently frequent, as indicated by comparison with test runs in which the updating is done every ten days. The non-photochemical sources and sinks are assumed to be time independent, and modeled as constant release rates or destruction coefficients over the appropriate types of surfaces.

Each experiment starts with a uniform distribution of CO, with a volume mixing ratio equal to 1×10^{-7}. The tracer model is usually run for four years, repeatedly using one year's data generated by the general circulation model. That the tracer model has reched steady state in the fourth year is indicated by the lack of further change in the global CO distrubtions between the third and fourth year. An a posteriori check on the mass balance in the tracer model reveals that it conserves mass to better than 1% per year, which is adequate for the present investigations.

Photochemical production and loss rates in the troposphere are constructed, using the set of reactions shown in Table 1a. The zonally averaged CO distribution is used to generate photochemical equilibrium solutions for the free radicals OH, HO_2, H_2O_2, $O(^1D)$, NO and NO_2. Distributions of water vapor mixing ratios and temperatures are taken from the general circulation model. Ozone concentrations and their seasonal variations are taken from the observations of Hering and Borden (1964). The concentrations of CH_4 and H_2 are set equal to 1.4 and 0.5 ppm, respectively, throughout the troposphere. The distribution of NO_x ($NO + NO_2$) is taken from Crutzen and Fishman (1977), with surface values of 0.1 ppb at 40°N and northward and 0.05 ppb southward, along with a scale height of 2 km. Because

of a lack of data, no seasonal variations are prescribed for the NO_x concentrations. The diurnally-averaged photodissociation rates are calculated in the usual way, with corrections for Rayleigh scattering (Yung et al., 1980). The effect of cloud cover is approximated, by dividing all dissociation rates in the lower troposphere below the cloud heights (5 km) by a factor of 2, since the average cloud cover is about 50%.

In arriving at the simplified chemistry shown in Table 1a we used several approximations regarding the interactions between the hydroxyl radicals, nitrogen oxides and methane-derived radicals. Since we fix total NO_x ($= NO + NO_2$), the only $HO_x - NO_x$ couplings are via the ratio,

$$\frac{NO}{NO_2} = \frac{J_2}{k_{17}[HO_2] + k_8 [O_3]} \tag{1}$$

and the formation of nitric acid,

$$NO_2 + OH + M \rightarrow HNO_3 + M \quad . \tag{R12}$$

Since the primary fate of HNO_3 formed in (R12) is loss by rainout, it is a good approximation to assume that (R12) is a sink for HO_x. The coupling between HO_x and radicals derived from the oxidation of methane is more complicated. We note that to an excellent approximation the destruction of each CH_4 molecule leads to the production of one H_2CO molecule. Hence, the net result of methane chemistry on HO_x can be parameterized by the following expressions,

$$P(H) = J_4 [H_2CO] = \gamma_2 [OH] \tag{2}$$

$$P(HO_2) = k_{20} [H_2CO] [OH] + J4 [H_2CO] = \gamma_1 [OH]^2 + \gamma_2 [OH] \tag{3}$$

$$L(OH) = k_{20} [H_2CO] [OH] = \gamma_1 [OH]^2 \tag{4}$$

where

$$\gamma_1 = k_{20}\, k_{16} [CH_4] / (J_4 + J_5 + k_{20} [OH])$$

$$\gamma_2 = J_4\, \gamma_1 / k_{20}$$

and P(x) and L(x) denote the production and loss rate ($cm^{-3}\ s^{-1}$) for species x respectively.

With these approximations we can calculate the photochemical equilibrium concentrations of the hydroxyl radicals (H, OH, HO_2 and H_2O_2) by balancing the production and loss rates for these radicals, as given in Table 1a and expression (2)-(4). This involves solving four simultaneous equations. However, noting that

$$[H] = \frac{k_{18} [CO] + k_{19} [H_2] + \gamma_2}{k11 [O_2] M} [OH] \tag{5}$$

and

$$[H_2O_2] = \frac{k_{14}}{J_3 + k_{15}[OH] + J_{22}} [OH_2]^2 \qquad (6)$$

further simplifies the mathematics to seeking the solution for only two non-linear algebraic equations in two unknowns (OH and HO_2). The solution is then used to improve the estimate of NO/NO_2 by (1). This procedure converges in a few iterations to better than 10^{-4}. Table 1b gives a representative example of the concentrations of important radical species calculated by this simplified chemical model. The approximate scheme (1)-(6) calculates HO_x concentrations that are within 10% of those computed, using the exact scheme given in Table 1a.

The stratospheric photochemical contributions are taken from two-dimensional model calculations using the reaction scheme of Yung et al. (1980), in which the latitudinal distribution of the long-lived species (Cl_x, NO_x, CH_4, etc.) are prescribed by projecting the one-dimensional model results along preferred mixing surfaces, (McElroy et al., 1976). The distribution of stratospheric water vapor is taken from Wofsy (1976).

Experiments

To investigate the CO sources and sinks, as well as the value of the mean tropospheric OH concentration, we performed eight experiments incorporating a wide range of production and loss mechanisms. These experiments are listed in Table 2, and are discussed below.

In experiment T1 we included an anthropogenic source of 6.3×10^{14} g/yr, (Seiler, 1974), distributed over land areas in proportion to energy consumption, (Darmstadter et al., 1971). No seasonal variation in the anthropogenic source was included as this effect is thought to be small (Hall et al., 1975). We also included a source from methane oxidation and a sink due to OH oxidation of CO. Both processes were distributed throughout the troposphere and stratosphere.

Tracer experiment T2 was the same as T1 except that the source from methane oxidation and loss by reaction with OH radicals were both arbitrarily reduced after each calculation to ensure a mean global abundance close to observed. This was done to determine the sensitivity of the model to the OH value.

Experiment T3 included, in addition to the sources and sinks used in T1, a plant source with a magnitude of 4.3×10^{14} g/yr, equal to the minimum estimate of Zimmerman et al. (1978), while their upper limit of 1.3×10^{15} g/yr, was used in T4. The latitudinal distribution of these sources was also taken from Zimmerman et al. for both experiments. Although the equatorial ground source has been parameterized by using values estimated by Zimmerman et al. (1978) for NMHC oxidation, there are other possibilities. For example, Crutzen et al. (1979) have suggested that the burning of vegetation either by forest fires or slash and burn agricultural practices, which are concentrated mainly in the tropics, might be a large CO source.

In experiment T5, we used the anthropogenic source and included the methane oxidation source and OH oxidation sink only in the stratosphere, to investigate the importance of transport to the stratosphere as a sink, (Newell, 1977), and to isolate the effects of tropospheric photochemistry. Based on previous experience with this combination, we anticipated that an additional loss term would be necessary, thus, in experiment T6 we parameterized a soil sink by using a deposition velocity of 4×10^{-2} cm/sec, as estimated by Liebl and Seiler (1976).

In experiment T7, we incorporated an ocean source, which is presumably associated with marine biological activity. While estimates of a potential oceanic source vary widely, we have used the (conservative) value of 0.4×10^{14} g/yr, estimated by Seiler and Schmidt (1975), which was distributed uniformly over the oceans.

Finally, in experiment T8 we included the same sources as in T4, except that the anthropogenic source was excluded in order to investigate the impact of anthropogenic releases on the global distribution.

The classification of sources into three groups--anthropogenic, CH_4 oxidation and plant--is somewhat arbitrary and is done solely for convenience. For instance, there would be a large anthropogenic component in the plant source, if a major component of that was due to slash and burn agricultural practices.

Results and Discussion

Figs. 2a and b depict vertically and zonally averaged CO concentrations as a function of latitude for the eight experiments, along with the observed values, (after Seiler, 1974). The experiment which produced the best fit was T4, which employed a maximum value of the plant source in addition to the anthropogenic and CH_4 oxidation sources. All the other experiments resulted in values lower than observed except for T5, which, without any tropospheric chemistry, produced values twice as large as observed. Unless the transport to the stratosphere is substantially underestimated, this result indicates that the stratosphere is not an important sink. When the soil sink was added, as in T6, it reduced the concentration to a value less than observed. Obviously it would be possible to "tune" the deposition velocity by varying it within the uncertainty range of Liebl and Seiler (1975), and therefore definitive conclusions about the strength of a soil sink can not be drawn from this experiment alone. However, as will be discussed later, the isotopic concentration of CO can be used to set constraints on the magnitude of the soil sink (Stevens et al., 1972). One can see that the experiments which lack any tropospheric chemistry, such as T5 and T6, or have reduced chemistry, such as T2, produce NH/SH ratios which differ from the observed by 20% or more. The qualitatively similar latitudinal distributions for T4 and T5 have different causes. In T4, the CO in the southern hemisphere is governed mainly by local sources and sinks (cf. Fig. 5a). In T5, CO rich air from northern mid latitudes is entrained into the rising branch of the Hadley circulation and is transported into the stratosphere, where it is destroyed. Stratospheric air which is poor in CO may then enter the mid-latitude southern hemisphere. In both cases, CO rich air is transported southward and upward by

the northern hemispheric branch of the Hadley circulation and CO poor air is transported northward and upward by the southern hemispheric branch, resulting in a sharp interhemispheric gradient at low altitudes. T8, which does not include an anthropogenic source, has a poor interhemispheric difference. The latitudinal asymmetry in T8 reflects the greater portion of land areas in the northern hemispheric tropics relative to the southern hemisphere. T8 may also describe the global CO distribution in the preindustrial atmosphere. The important assumptions and results of experiments T1-T8 are summarized in Table 3.

The computed seasonal variations of CO at 55°N is shown in Figs. 3a and 3b along with observations at Zvenigorod, USSR (Dianov-Klokov et al., 1978). Figs. 3c and 3d show the model derived seasonal variations at 20°N. The data is based on the observations of Seiler et al. (1976) at Mauna Loa. Both data sets were shown to be relatively free of local pollution influences, and should be representative of conditions in the clean troposphere. In general, all the models which had reduced OH levels in the troposphere could not satisfactorily reproduce the observed seasonal variation at 50°N, both in amplitude and phase.

The observations of CO at 55°N and 20°N show little or no phase difference. This behavior is in striking contrast to the seasonal variations of CO_2, which show significant differences between latitude belts, (Junge and Czeplak, 1968). The seasonal variations of CO_2 are driven mainly at high latitudes; at high northern latitudes the minimum occurs in late summer, which is six months different from the southern hemispheric summer minimum. At low northern latitudes, with the intrusion of air from the southern hemisphere, the phase is delayed. However, the observed seasonal variations of CO appear to be driven uniformly with latitude, indicating a shorter lifetime and a dominance of local sources and sinks. This is consistent with seasonal variations in the OH concentration as the primary mechanism responsible for the seasonal variations of CO. The concentration of OH depends strongly on the duration and intensity of UV sunlight. Model derived OH values showed little or no variation in the times when maximum or minimum concentrations occur at different latitudes. The seasonal variations of CO observed by Seiler et al. (1976) and Dianov-Klokov et al. (1978) likewise showed no difference in phase, a difference which would have been expected if the seasonal forcing were to arise from some feature such as a seasonal variation in the anthropogenic input.

If the seasonal CO data are accurate this suggests that local chemistry may be more important and the atmospheric OH may be even higher than it is in the model. We have examined the sensitivity of the results in a model in which the OH concentrations were increased by one third over the values in T4. The results showed that both the amplitudes and phases of the seasonal variations were in much better agreement with observations. Alternatively, there may be a seasonal variation in the strength of the low latitude source. As there is little seasonality in primary productivity in tropics, which is dominated by rain forests, we would expect no seasonal variation in the strength of the tropical source, if the scaling of hydrocarbon emissions to productivity used by Zimmerman et al. (1978) is adopted. There may be a seasonal variation in the CO source derived from vegetation burning. In the northern hemispheric tropics the dry season is in winter (Richards, 1979). Enhanced forest fires in this season would contribute a source that could improve the comparison between the model and observations.

T5 and T6, which do not include tropospheric chemistry, have little seasonal variation. T2, with reduced chemistry, has a seasonal variation somewhat smaller than observed. The comparisons in Figs. 2-3 imply that both tropospheric chemistry and the anthropogenic source are necessary components of the CO budget.

We also investigated the latitude-height distribution of CO. Fig. 4 shows an estimate of the observed distribution, (Seiler, 1974). The low level maximum at upper mid-latitudes presumably due to the anthropogenic source, is apparent, as is a lower latitude upper tropospheric bulge in the CO isopleths. At 10°S, values increase by more than 75% between the surface and 12 km. All the model experiments fail to produce this feature except for T3 and T4, the experiments which include the plant CO source. Fig. 4b shows the result from year 4 for T2. The omission of a low latitude source is primarily responsible for the absence of the equatorial bulge in this model. Fig. 4c presents the results for T4. The upper tropospheric bulge is apparent as well as the maximum at high latitudes. The distribution above the tropopause is unrealistic due to the failure of a seven-layer model to adequately resolve the tropopause, and thus to accurately model troposphere-stratosphere exchange.

It is of interest to determine how the upper troposphere bulge is produced in T4. As indicated in the above discussion, T4 concentrations are largely produced locally and this is true for the vertical distribution as well. The biologically produced CO at low latitudes is transported vertically, mainly by the model's small scale convection, in agreement with the mechanism proposed by Falconer and Pratt (1980). Indication that a local ground source is responsible for the observed bulge comes from the high altitude measurements of Gauntner et al. (1979) of CO and Aitken nuclei over the tropics. Their results show that high CO concentrations are associated with high Aitken nuclei counts, indicating a common source for both of these quantities. The upper troposphere data of Seiler (1974) were taken over the Atlantic, and are similar to those observed by Gauntner et al. (1979) over Africa. In addition, the data of Gauntner et al. show higher values at equatorial latitudes over Africa than over the Pacific. The results of T4 are consistent with these observations. The longer distance from the major northern hemispheric source regions result in lower values over the equatorial Pacific. In T2, the longer lifetime of CO allows for its more complete redistribution around the globe. The Gauntner et al. data were obtained on only one flight, so more data are needed to check if these are persistent features of the CO distribution, and to examine the seasonal variability of the interhemispheric transport of CO.

Based on the complete set of experiments, we conclude that T4 is the most successful combination of sources and sinks for simulating the observed CO distribution. A more detailed analysis of T4 and its comparison with T2 will now be given. The continuity equation may be written as:

$$\frac{\delta M}{\delta t} = H + V + P - L + S \qquad (7)$$

where M is the mass of tracer, H the horizontal convergence associated with transport by eddies and the mean circulation, P and L the chemical production and loss terms, V the vertical transport into the troposphere from the stratosphere, and S the ground source. The results are shown in Fig. 5a and 5b for T4 and T2, to emphasize the roles of the various terms in different experiments. T4 and T2 have somewhat similar latitudinal distributions as shown in Fig. 2a, yet the additional source in T4, and the reduced chemistry in T2 result in the distributions being produced by different mechanisms. In T4 much of the CO is governed by a local cycle of sources and sinks, with the concentration peaking where the sources are a maximum and in the intervening 30° latitude belt, where the horizontal convergence from the neighboring zones is significant. In T2, the distribution at lower latitudes is more strongly influenced by the horizontal convergence. In this case, the long lifetime of CO allows for its long range advection, but in so doing it also reduces much of its variability.

The results of these experiments imply that the globally averaged OH concentration is approximately 7×10^5 cm^{-3}. (Singh (1977) has used observations of the interhemispheric difference of methyl chloroform (CH_3CCl_3) to deduce globally averaged OH concentrations of at most 4×10^5 cm^{-3}. However, two recent studies, Jeong and Kaufman, 1979; Kurylo et al., 1979), using independent techniques, have derived a revised rate coefficient for the reaction CH_3CCl_3 + OH. This value is about a factor of two lower than that used by Singh in his analysis. These new results imply that his derived OH concentrations should be increased by a factor of two and are consistent with values obtained in experiment T4. Isopleths of the mean concentrations of OH in units of 10^5 molecules cm^{-3} for the month of January and July computed in experiment T4 are shown in Figures 6a, b. These results for OH are in good agreement with those derived recently by Volz et al. (1981) on the basis of ^{14}CO studies.

Experiment T8 is designed to reconstruct the state of the atmosphere of the pre-industrial era. The input parameters for T8 are the same as those for T4 except for the industrial source, which is set equal to zero. A comparison between T4 and T8 suggests that there may have been a 65% change in the northern hemispheric CO concentration due to industrial pollution and a much smaller change in the southern hemisphere. Indeed, a comparison between Shaw's (1958) data taken in Ohio during 1952-1953 and Dianov-Klokov's data in the 1970's in the USSR indicates that there might have been a substantial increase in the CO concentration during this period. The mean value of OH in T8 is about 20% higher than that in T4, which suggests that there has been an increase in the tropospheric lifetimes of species such as CH_4, CH_3Cl, CH_3Br and $CHCl_3$. In our current investigation we have fixed the concentrations of CH_4 and NO_x at present atmospheric levels. If we had fixed the source strength of CH_4, the shorter lifetime would have implied an increase of CH_4 concentration in the atmosphere. Indeed, the recent observations by Rasmussen et al. (1981) provide strong evidence for an increase in atmospheric CH_4. We have not conducted extensive studies on the sensitivity of our chemical model to inputs such as NO_x and O_3. The primary objective of this paper is to derive OH concentrations from the behaviour of CO in the model atmosphere. This study is, therefore, more like a diagnostic study of CO and OH than a prognostic one. We regard the observed distributions of O_3 and NO_x as useful constraints in construction of chemical time constants for CO. It is precisely because of the uncertainties in the NO_x and O_3 abundances, in the

rate coefficients for key reactions, and in the heterogeneous loss rates that we have adopted the current approach: a self-consistent study of the spatial distribution and temporal variations of CO and HO, to go beyond the current immediate objective would be difficult to justify.

Global measurements of the $^{18}O/^{16}O$ ratio of CO by Stevens et al. (1972) typically show values much lower than are derived from the incomplete combustion of fossil fuels. Fractionation by destruction mechanisms cannot be invoked to explain the data. Loss by reaction with OH radicals, R20, would favor the lighter isotope (Weinstock and Chang, 1974). Stevens et al. (1972) have measured the fractionation in CO consumption by soil bacteria and found that it favors the lighter isotopes. All of their northern hemispheric measurements indicate a predominance of light isotopic species during the summer when soil scavenging would be at its maximum, which is contrary to what would be expected if the soil were acting as a major sink. It would also be difficult to explain the data by assuming equilibrium of CO with respect to uptake and release by the soil. By analogy with CO_2, release from the soil and from plants may involve no fractionation, or again favor the lighter isotope (Keeling, 1973).

The models which do not include vegetation sources have difficulty in explaining the isotopic pattern found in the northern hemisphere, as they predict northern hemispheric CO to be mainly anthropogenic throughout the year. Experiment T6, which assumes the only sink to be soil scavenging is also inconsistent with the Stevens et al. (1972) results as the CO in the northern hemisphere would be even heavier than that released from combustion. As mentioned previously, the seasonal pattern of the $^{18}O/^{16}O$ ratio would be exactly opposite to what is observed. These results are consistent with the view that the soil plays a relatively minor role in the CO cycle.

Since carbon-13 values from fossil fuel CO overlap those from natural sources, these measurements may not be particularly useful as a diagnostic of source types. Measurements of carbon-14, on the other hand, might be more useful. The use of carbon-14 and oxygen-18 data would then minimize the uncertainties due to mixing of air masses. Figure 7 shows the annually averaged concentrations contributed by each of the sources we have included in experiment T4. They were derived by using each source separately with the OH field derived by T4 to determine the loss rate. The figure shows that virtually none of the anthropogenic CO emitted in the northern hemisphere reaches the southern hemisphere. The results also show that a sizeable fraction of the CO at mid to high northern latitudes is not anthropogenic. Our results are in qualitative agreement with the major conclusions reached by Weinstock and Niki (1972) and Stevens et al. (1972). More definitive statements cannot be made until more clean air measurements are available. The two sets of measurements reported above were subject to local anthropogenic influences.

Conclusions

In this paper, we have examined an extensive set of experiments in the search for an understanding of four major features of atmospheric CO: (1) the meridional distribution, (2) the seasonal variation, (3) the equatorial bulge, and (4) the isotopic composition. The results demonstrate the power and versatility of the general circulation model approach, as compared with more

traditional analyses (Wofsy, 1976; Crutzen & Fishman, 1977; Hameed and Stewart, 1979). The most successful experiment, T4, which reproduces all the essential observed features, requires, in addition to anthropogenic and CH_4 oxidation sources, a large surface source of order 1.3×10^{15} g/yr^{-1}. This additional source must span the low latitudes in the Hadley cell regime, in order to produce the observed equatorial bulge.

Our model is consistent with a globally averaged OH concentration of about 7×10^5 cm^{-3}. At this OH level, we are able to simulate the main features of the seasonal variation, observed by Dianov-Klokov et al. (1978) in Zvenigorod (55°N). The seasonal data obtained by Seiler et al. (1976) at Mauna Loa (20°N) implies an even higher concentration of OH at lower latitudes than that in our T4 experiment or, alternatively, a possible seasonality in the plant source. The concentration of OH cannot, however, significantly exceed that calculated in T4, based on our current understanding of the CH_3CCl_3 distribution (Singh, 1977; Chang and Penner 1978; Jeong and Kaufman, 1979; Kurylo et al., 1979). We are planning a general circulation model study of CH_3CCl_3 with a 12-layer model in order to make an independent investigation of tropospheric OH.

No doubt a different and perhaps more elaborate combination of sources and sinks and OH concentrations could also reproduce the observed features of CO. However, the model has been constructed with the fewest number of assumptions possible, and within the current small set of assumptions we are confident of the uniqueness of our results. We expect to improve and refine our models as more CO measurements become available.

Measurements of the isotopic content of the CO formed by various mechanisms such as vegetation burning, the oxidation of hydrocarbons such as isoprenes and terpenes could be valuable in estimating the relative roles of these processes. Measurements of the seasonal variations of the total CO concentrations, and their isotopic composition at remote locations could be used with data on the source characteristics to further quantify the magnitudes of the sources involved. Locations already in use for monitoring CO_2, N_2O and chlorofluorocarbons could be used for this purpose. Because the intertropical convergence zone may be weaker over the Pacific than the Atlantic (Atkinson and Sandler, 1970), it should present less of a barrier to interhemispheric exchange and local sources in determining seasonal cycles and interhemispheric gradients of CO and other tracers in existing Pacific sites at the same latitudes.

References

Atkinson, G., and J. Sandler, Mean cloudiness and gradient level wind charts over the tropics, Tech. Rept. #215, Air Weather Service, USAF, Scott AFB, Illinois, 1970.

Bates, D.R., and A.E. Witherspoon, The photochemistry of some minor constituents of the earth's atmosphere, Monthly Notices Roy. Astron. Soc., 112, 101-124, 1952.

Chang, J.S., and J.E.P. Penner, Analysis of global budgets of halocarbons, Atmos. Environ., 12, 1867-1873, 1978.

Crutzen, P.J., and J. Fishman, Average concentrations of OH in the troposphere and the budgets of CH_4, CO, H_2 and CH_3CCl_3, Geophys. Res. Lett., 4, 321-324, 1977.

Crutzen, P.J., L.E. Heidt, J.P. Krasnec, W.H. Pollack, and W. Seiler, Biomass burning as a source of atmospheric gases CO, H_2, NO, CH_3Cl, and COS, Nature, 282, 253-256, 1979.

Darmstadter, J., P.D. Teitelbaum and J.G. Polach, Energy in the World Economy: A Statistical Review of Trends in Output, Trade, and Consumption since 1925. Johns Hopkins Press, Baltimore, 876 pp., 1971.

Dianov-Klokov, V.I., Ye. V. Fokeyeva, and L.N. Yurganov, A study of the carbon monoxide content of the atmosphere. Izvestiya, Atm. and Ocean Phys., 14, 263-270, 1978.

Falconer, P. and R. Pratt, Comments on "Experimental Guidance for Interhemispheric Transport for Airborne Carbon Monoxide Measurements", J. Appl. Meteorol., 19, 338-339, 1980.

Gaunter, D.J., T. Nyland, M. Tiefermann, and T. Dudzinski, Measurements of carbon monoxide, condensation nuclei, and ozone on a B 747SP, Geophys. Res. Lett., 6, 167-170, 1979.

Hall, C.A.S., C.A. Edkahl, and D.E. Wartenberg, A fifteen-year record of biotic metabolism in the Northern Hemisphere, Nature, 255, 136-138, 1975.

Hameed, S., and R.W. Stewart, Latitudinal distribution of the sources of carbon monoxide in the troposphere, Geophys. Res. Lett., 6, 841-844, 1979.

Hansen, J.E. et al., An efficient three-dimensional global model for climate studies, to be submitted to J. Atmos. Sci.,

Hering, W.S., and T.R. Borden, Ozonesonde observations over North America, Doc. AFCRL-64-30 (1, 2), U.S. Air Force Cambridge Res. Lab., Bedford, Mass., 1964.

Hochanadel, C.J., J.A. Ghormley and P.J. Ogren, Absorption spectra and reaction kinetics of the HO_2 radical in the gas phase, J. Chem. Phys., 56, 4426-4432, 1972.

Jeong, K.-M., and F. Kaufman, Rates of the reactions of 1,1,1-Trichloroethane 1,1,2-Trichloroethane with OH, Geophys. Res. Lett., 6, 757-759, 1979.

Junge, C. and G. Czeplak, Some aspects of the seasonal variation of carbon dioxide and ozone, Tellus, 20, 422-434, 1968.

Keeling, C.D., The carbon dioxide cycle: Reservoir models to depict the exchange of atmospheric carbon dioxide with the ocean and land plants, in Chemistry of the Lower Atmosphere, S.I. Rasool (ed.), Plenum Press, New York, 1973.

Kurylo, M.J., P.C. Anderson, and O. Klais, A flash photolysis resonance fluorescence investigation of the reaction OH + CH_3CCl_3 + H_2O + CH_2CCl_3, Geophys. Res. Lett., 6, 760-762, 1979.

Levy, H. II, Normal atmosphere: large radical and formaldehyde concentrations predicted, Science, 173, 141-143, 1971.

Liebl, K.H., and W. Seiler, CO and H_2 destruction at the soil surface, in Microbial Production and Utilization of Gases, eds. H.G. Schlegel, G. Gottschalk, and N. Pfenning, 1976.

Logan, J.A., M.J. Prather, S.C. Wofsy, and M.B. McElroy, Atmospheric chemistry: response to human influence, Phil. Trans. Roy. Soc. A290, 187-234, 1978.

Mahlman, J.D., and W.J. Moxim, Tracer simulation using a global general circulation model: results from a mid-latitude instantaneous source experiment, J. Atmos. Sci., 35, 1340-1374, 1978.

Mahlman, J.D., and R.W. Sinclair, Tests of various numerical algorithms applied to a simple trace constituent air transport problem in Fate of Pollutants in the Air and Water Environment, (ed.) I.H. Suffet, Wiley, New York, pp. 223-252, 1977.

McConnell, J.C., M.B. McElroy, and S.C. Wofsy, Natural sources of atmospheric CO, Nature, 233, 187-188, 1971.

McElroy, M.B., J.W. Elkins, S.C. Wofsy, and Y.L. Yung, Sources and sinks for atmospheric N_2O, Rev. of Geophys. and Space Phys., 14, 143-150, 1976.

Migeotte, M.V., The fundamental band of carbon monoxide at 4.7μ in the solar spectrum, Phys. Rev., 75, 1108-09, 1948.

NASA RP-1010, Chlorofluoromethanes and the stratosphere, ed. R.D. Hudson, 266pp., 1977.

NASA, Chemical kinetic and photochemical data for use in stratospheric modeling. Evaluation No. 2 NASA Panel for Data Evaluation, JPL79-27, Jet Propulsion Laboratory, 266pp., 1979.

Newell, R., One-dimensional models: a critical comment, and their application to carbon monoxide, J. Geophys. Res., 82, 1449-1450, 1977.

Rasmussen, R.A. and M.A.K. Khalil, Atmospheric methane (CH_4): trends and seasonal cycles, EOS, 62, #27, 1981.

Richards, P.W., The Tropical Rain Forest, Cambridge Univ. Press, 450 pp., 1979.

Russell, G.L., and J.A. Lerner, A new finite difference scheme for three dimensional advection, to be published in J. Comp. Phys., 1981.

Seiler, W., The cycle of atmospheric CO, Tellus, 26, 116-135, 1974.

Seiler, W., H. Giehl, and H. Ellis, A method for monitoring of background CO and first results of continuous CO registrations on Mauna Loa Observatory, Special Env. Report No. 10, WMO, no. 460, Geneva, Switzerland, 1976.

Seiler, W., and U. Schmidt, New aspects of CO and H_2 cycles in the atmosphere, Proc. Int. Conf. on Structure, Composition, General Circulation of Upper and Lower Atmospheres and Possible Anthropogenic Perturbations, JAMAP, 192-222, 1974.

Shaw, J.H., The abundance of atmospheric carbon monoxide above Columbus, Ohio. Astrophys. J., 128, 428-40, 1958.

Singh, H.B., Atmospheric halocarbons: Evidence in favor of reduced average hydroxyl radical concentration in the troposphere, Geophys. Res. Lett., 4, 101-104, 1977.

Stevens, C.M., L. Krout, D. Walling, A. Venters, A. Engelkemeir, and L.E. Ross, Isotopic composition of atmospheric carbon monoxide, Earth & Planet. Sci. Lett., 16, 147-165, 1972.

Sze, N.D. Anthropogenic CO emissions: Implications for atmospheric CO-OH-CH_4 cycle, Science, 195, 673-675, 1977.

Volz, A., D.H. Ekhalt and R.G. Derwent seasonal and latitudinal variation of ^{14}CO and the tropospheric concentration of OH radicals, J. Geophys. Res., 86, 5163-5171, 1981.

Weinstock, B., and T.Y. Chang, The global balance of carbon monoxide, Tellus, 26, 108-115, 1974.

Weinstock, B., and N. Niki, Carbon monoxide balance in nature, Science, 176, 290-292, 1972.

Wofsy, S.C., Interactions of CH_4 and CO in the earth's atmosphere, Ann. Rev. Earth and Plan. Sci., 4, 441-470, 1976.

Yung, Y.L., M.B. McElroy, and S.C. Wofsy, Atmospheric halocarbons: A discussion with emphasis on chloroform., Geophys. Res. Lett., 2, 397-399, 1975.

Yung, Y.L., J.P. Pinto, R.T. Watson, and S.P. Sander, Atmospheric bromine and ozone perturbations in the lower stratosphere, J. Atmos. Sci., 37, 339-353, 1980.

Zimmerman, P.R., R.B. Chatfield, J. Fishman, P.J. Crutzen, and P.L. Hanst, Estimates of the production of CO and H_2 from the oxidation of hydrocarbon emissions from vegetation., Geophys. Res. Lett., 5, 679-681, 1978.

Table 1a. Reactions used for the calculation of OH concentration in the photchemical model. Two-and three-body rate coefficients are given in units of cm^3s^{-1} and cm^6s^{-1}, respectively. The diurnally-averaged mean dissociation rates and rainout rates, (in units s^{-1}), are given for spring equinox at 35°N, at the ground. The value shown for K12 is the two-body high pressure limit.

	Reaction	Rate Coefficient	Reference
R1	$O_3 + h\nu \rightarrow O_2 + O(^1D)$	$J1 = 1.92 \times 10^{-6}$	(a)
R2	$NO_2 + h\nu \rightarrow NO + O$	$J2 = 3.57 \times 10^{-3}$	(a)
R3	$H_2O_2 + h\nu \rightarrow OH + OH$	$J3 = 2.54 \times 10^{-6}$	(b)
R4	$H_2CO + h\nu \rightarrow HCO + H$	$J4 = 5.04 \times 10^{-6}$	(b)
R5	$H_2CO + h\nu \rightarrow H_2 + CO$	$J5 = 1.30 \times 10^{-5}$	(b)
R6	$O)^1D) + M \rightarrow O(^3P) + M$	$k6 = 4.0 \times 10^{-11}$	(b)
R7	$O(^1D) + H_2O \rightarrow OH + OH$	$k7 = 2.3 \times 10^{-10}$	(b)
R8	$NO + O_3 \rightarrow NO_2 + O_2$	$k8 = 2.1 \times 10^{-12}\ e^{-1450/T}$	(a)
R9	$OH + O_3 \rightarrow HO_2 + O_2$	$k9 = 1.5 \times 10^{-12}e^{-1000/T}$	(a)
R10	$HO_2 + O_3 \rightarrow OH + 2O_2$	$k10 = 1.5 \times 10^{-14}e^{-600/T}$	(b)
R11	$H + O_2 + M \rightarrow HO_2 + M$	$k11 = 1.8 \times 10^{-32}e^{+340/T}$	(c)
R12	$OH + NO_2 \rightarrow HNO_3$	$k12 = 1.15 \times 10^{-11}$	(a)
R13	$OH + HO_2 \rightarrow H_2O + O_2$	$k13 = 2.0 \times 10^{-10}$	(d)
R14	$HO_2 + JP_2 \rightarrow H_2O_2 + O_2$	$k14 - 2.5 \times 10^{-12}$	(b)
R15	$H_2O_2 + OH \rightarrow H_2O + HO_2$	$k15 - 1.0 \times 10^{-11}e^{-750/T}$	(b)
R16	$CH_4 + OH \rightarrow CH_3 + H_2O$	$k16 = 2.3 \times 10^{-12}e^{-1710/T}$	(b)
R17	$NO + HO_2 \rightarrow OH + NO_2$	$k17 = 4.1 \times 10\text{-}12e^{200/T}$	(b)
R18	$CO + OH \rightarrow CO_2 + H$	$k18 = 1.3 \times 10^{-13}(1 + P_{atm})$	(o)
R19	$H_2 + OH \rightarrow H_2O + H$	$k19 = 1.8 \times 10^{-11}e^{-2400/T}$	(b)
R20	$H_2CO + OH \rightarrow HCO + H_2O$	$k20 = 1.4 \times 10^{-11}$	(c)
R21	$HCO + O_2 \rightarrow CO + HO_2$	$k21 = 5.7 \times 10^{-12}$	(a)
R22	$H_2O_2 \rightarrow$ Rainout	$J22 = 2.0 \times 10^{-6}$	(e)

[a]NASA 1977. [b]NASA 1979. [c]Logan et al. (1978).

[d]Hochanadal (1972) and DeMore (personal communication, 1978).

[e]Wofsy, (1976).

Table 1b. A representative calculation of the major species in the simplified chemical model for March at 35°N at the ground. The kinetic rate coefficients are taken from Table 2a. All number densities are given in units of cm^{-3}.

Input to Chemical Model	Output from Chemical Model
$T = 281°K$	$[O^1D] = 1.66 \times 10^{-3}$
$M = 2.29 \times 10^{19}$	$[H] = 1.49 \times 10^{-1}$
$[H_2O] = 2.38 \times 10^{17}$	$[OH] = 5.93 \times 10^{5}$
$[O_3] = 8.4 \times 10^{11}$	$[HO_2] = 1.79 \times 10^{8}$
$[NO_x] = 1.55 \times 10^{9}$	$[H_2O_2] = 3.49 \times 10^{10}$
$[CO] = 4.35 \times 10^{12}$	$[NO] = 3.61 \times 10^{8}$
	$[NO_2] = 1.19 \times 10^{9}$

Table 2. Summary of sources and sinks used in the construction of the tracer models.

Experiment	Sources	Sinks
T1	Anthropogenic (a) CH_4 Oxidation (b)	CO + OH
T2	Anthropogenic (a) 1/2 CH_4 Oxidation (b)	1/2 (CO + OH)
T3	Anthropogenic (a) CH_4 Oxidation (b) Plant Source MIN (c)	CO + OH
T4	Anthropogenic (a) CH_4 Oxidation (b) Plant Source Max (d)	CO + OH
T5	Anthropogenic (a) CH_4 Oxidation Stratosphere (e)	CO + OH Stratosphere (e)
T6	Anthropogenic (a) CH_4 Oxidation Stratosphere (e)	CO + OH Stratosphere (e)
T7	Anthropogenic (a) CH_4 Oxidation (b) Ocean (g)	CO + OH
T8	CH_4 Oxidation (b) Plant Source Max (d)	CO + OH

(a) 6.3×10^{14} g/yr^{-1} (Seiler, 1974)

(b) based on OH calculated in the chemical model (see text).

(c) 4.3×10^{14} g/yr^{-1} distributed according to Zimmerman et al. (1978). However we do not distinguish between NMHC and vegetation burning sources.

(d) 1.3×10^{15} g/yr^{-1}, otherwise same as (c).

(e) These reactions take place in the stratosphere only. There is no tropospheric chemistry.

(f) deposition velocity over soil = 4×10^{-2} cms^{-1}.

(g) 4×10^{13} g/yr^{-1} (Seiler & Schmidt, 1975).

Table 3. Summary of results obtained from the eight tracer expieriments. CO concentrations are given in parts per billion by volume. Units for production and destruction mechanisms are 10^{14} g CO/yr. The abbreviation Ind. referes to industrial and NMHC to non-methane hydrocarbon.

Experiments	T1	T2	T3	T4	T5	T6	T7	T8	Observations
CO(ppb)	46	95	62	107	241	59	48	65	110
L(OH + CO, 10^{14}g/yr)	15	8.5	18.6	25.9	5.7	1.8	15.3	20.6	
P(CH_4 oxidation)	8.7	2.6	7.9	6.3	0.3	0.3	8.6	7.4	
P(Ind)	6.3	6.3	6.3	6.3	6.3	6.3	6.3	6.3	
P(NMHC)	—	—	4.3	13.1	—	—	—	13.1	
L(Soil)	—	—	—	—	—	4.8	—	—	
P(Ocean)	—	—	—	—	—	—	0.4	—	
OH(cm^{-3} x 10^{-5})	10.0	3.0	9.0	7.1	—	—	9.9	8.4	
CO(NH)/CO(SH)	2.6	3.0	2.5	2.3	1.8	3.4	2.5	1.3	2.5
OH(NH)/OH(SH)	0.7	0.7	0.7	0.7	—	—	0.7	0.8	

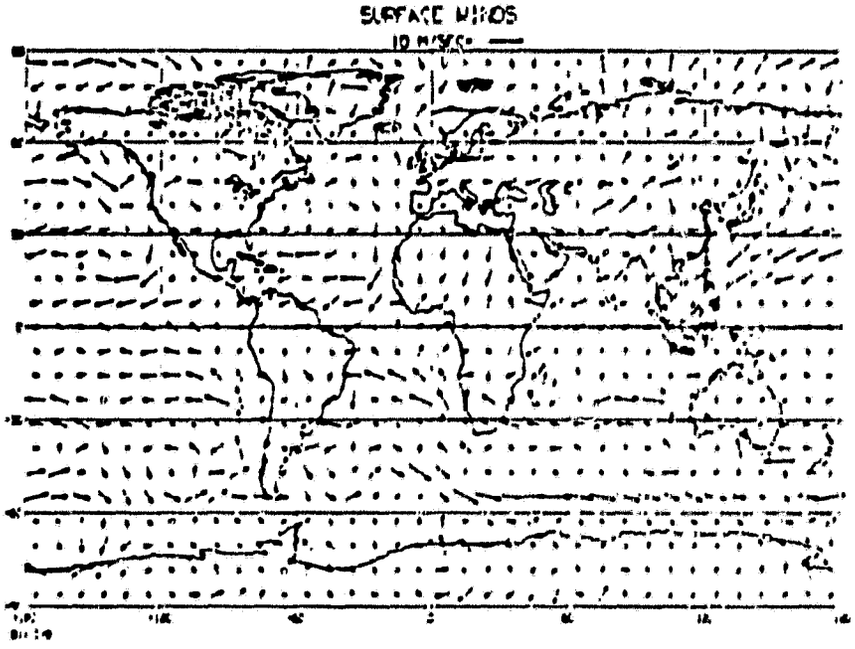

Figure 1a: Surface winds predicted by the general circulation model used for tracer studies for January.

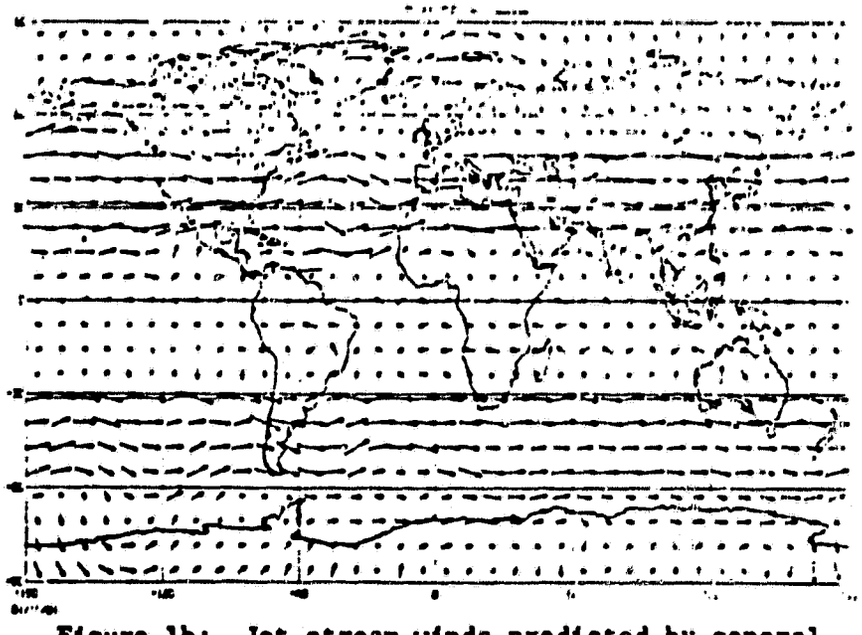

Figure 1b: Jet stream winds predicted by general circulation model for January.

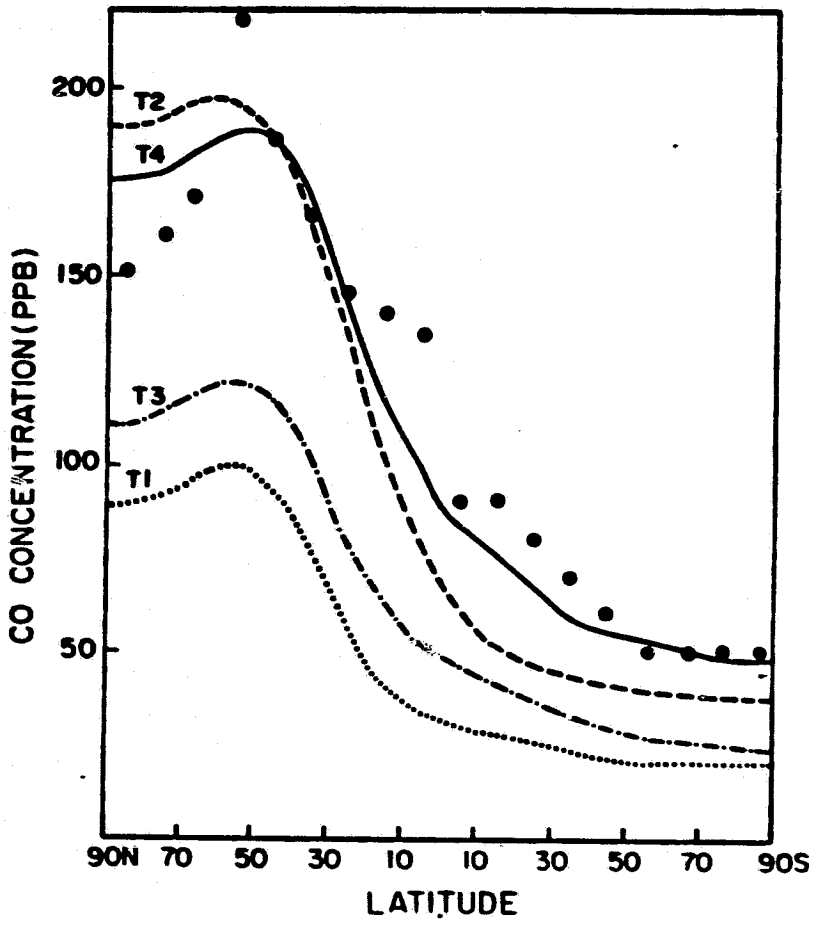

Figure 2a: Vertically and zonallly averaged CO concentrations as a function of latitude for tracer experiments T1-T4. Observations by Seiler, 1974 are shown as full circles.

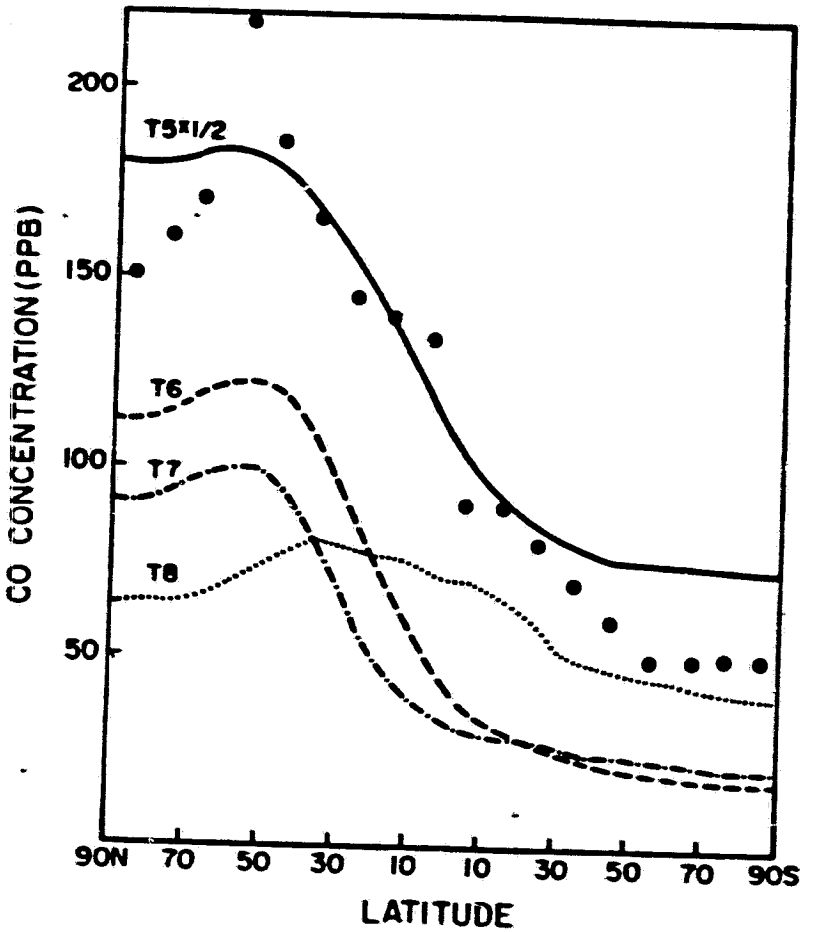

Figure 2b: Same as Figure 1a for tracer experiments T5-T8. Values shown for experiment T5 have been divided by two.

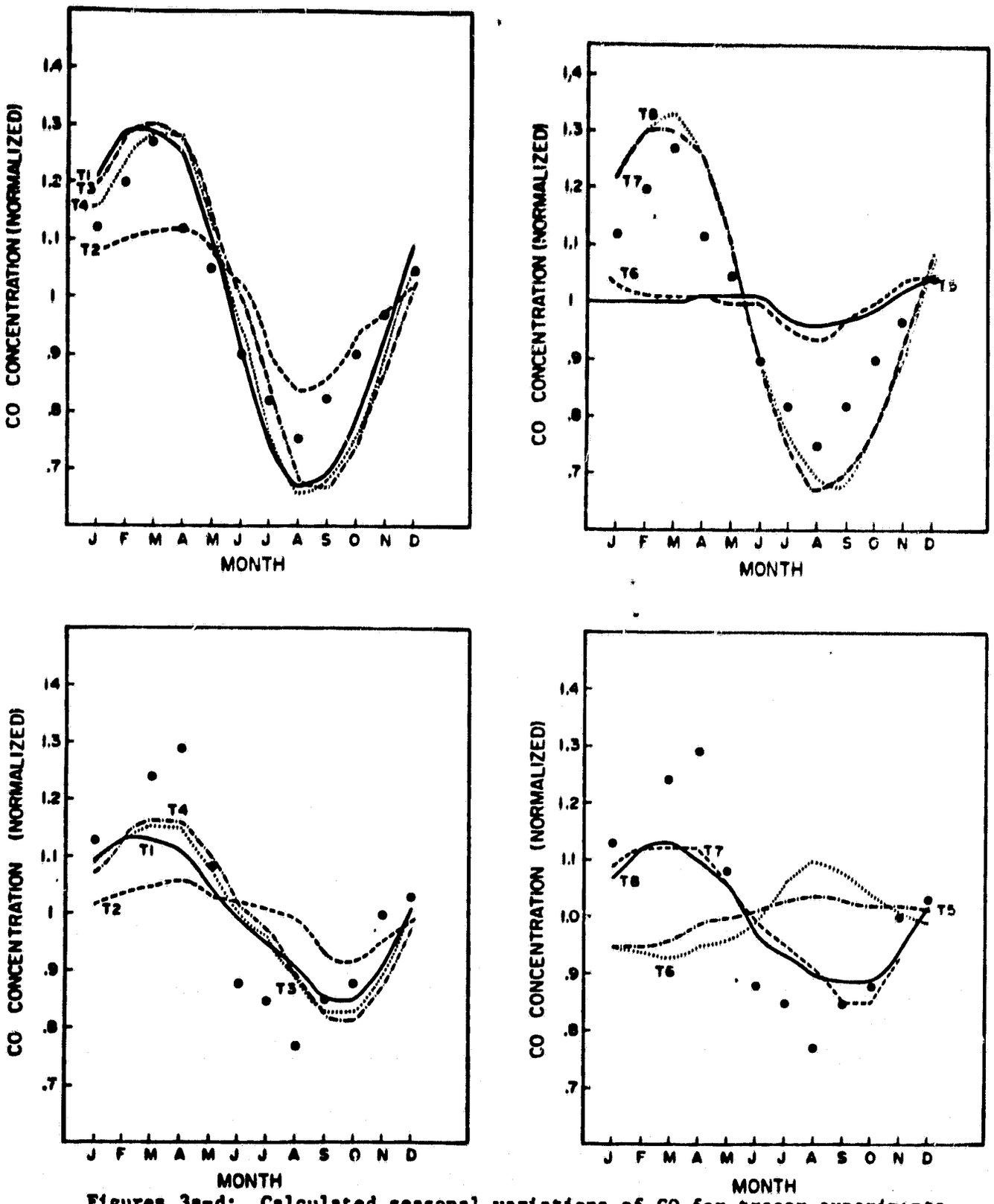

Figures 3a-d: Calculated seasonal variations of CO for tracer experiments a) T1-T4 at 55°N, b) T5-T8 at 55°N observed values by, Dianov-Klokov et al., 1978, c) T1-T4 at 20°N, d) T5-T8 at 20°N observed values by, Dianov-Klokov et al., 1978.

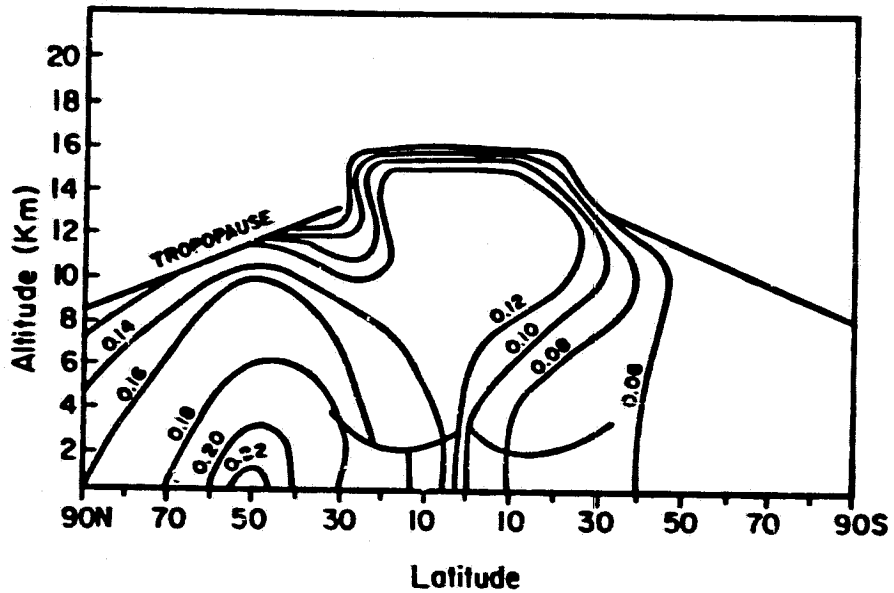

Figure 4a: Observed latitude-height contours of CO over the Atlantic Ocean (Seiler and Schmidt, 1974).

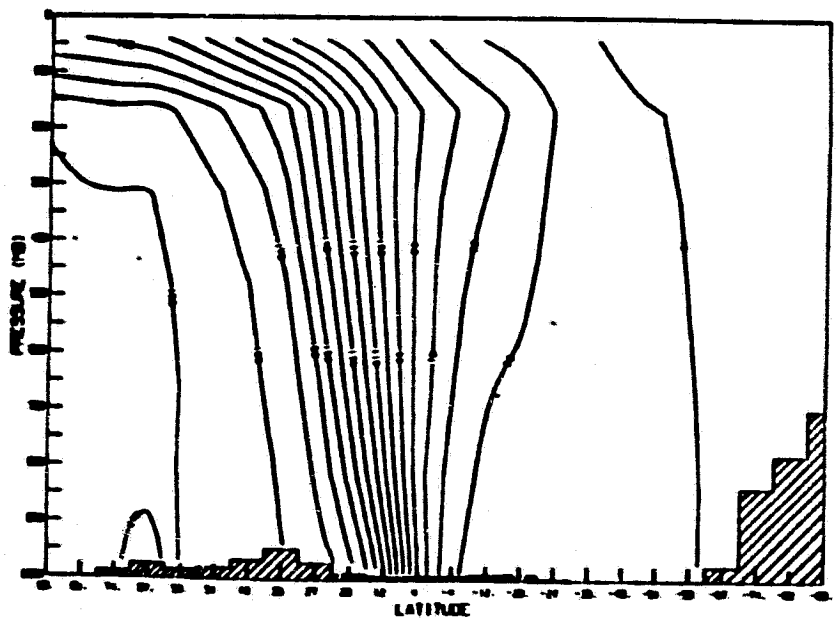

Figure 4b: Latitude-height contours over the Atlantic Ocean produced by experiment T2. Values shown are averaged over the last year of the model run.

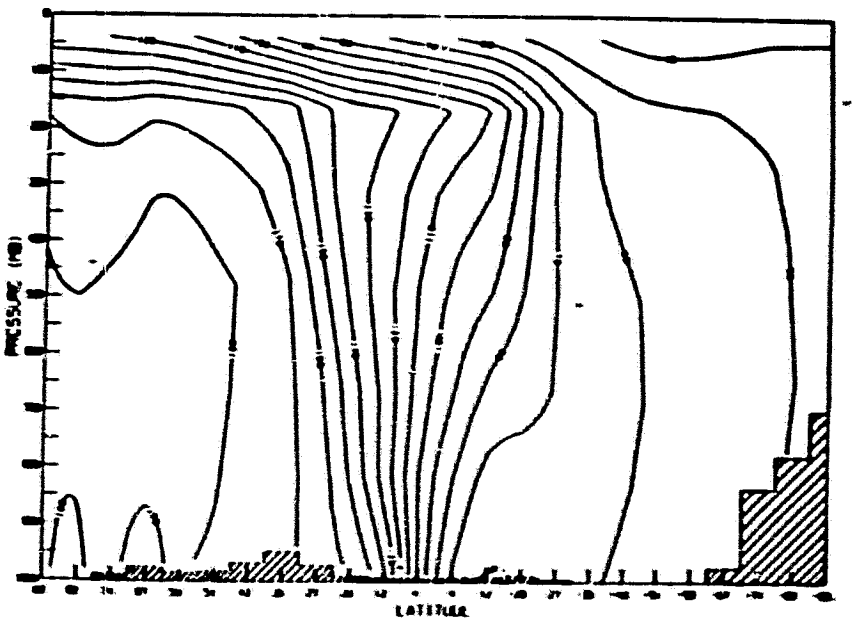

Figure 4c: Same 3b except for experiment T4.

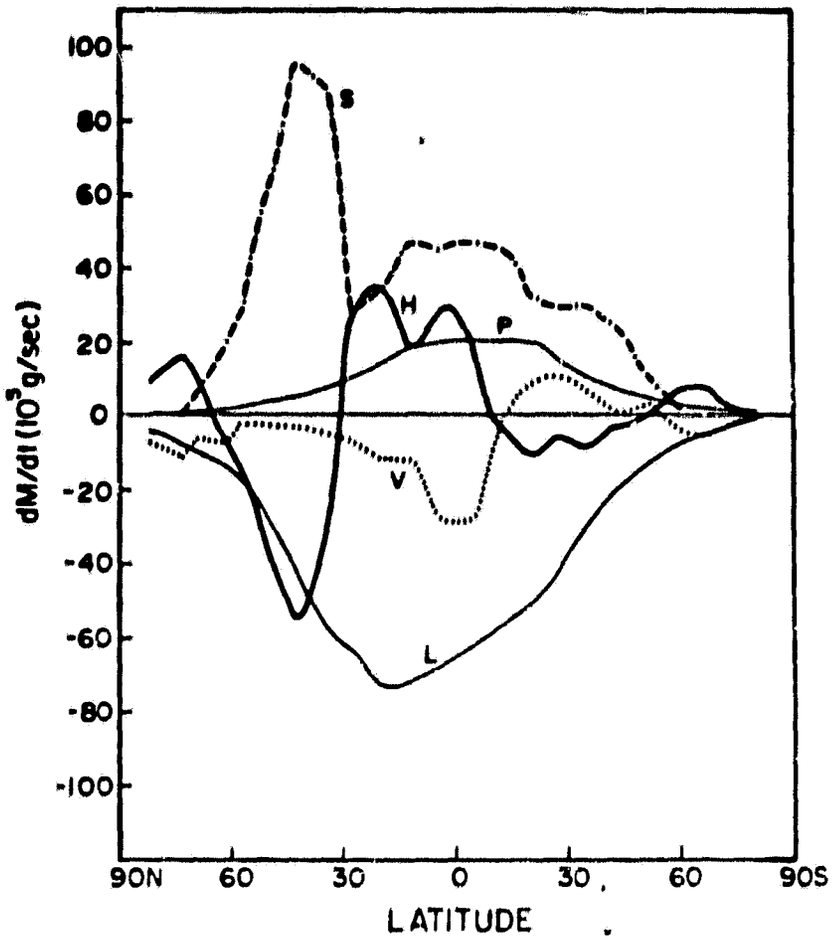

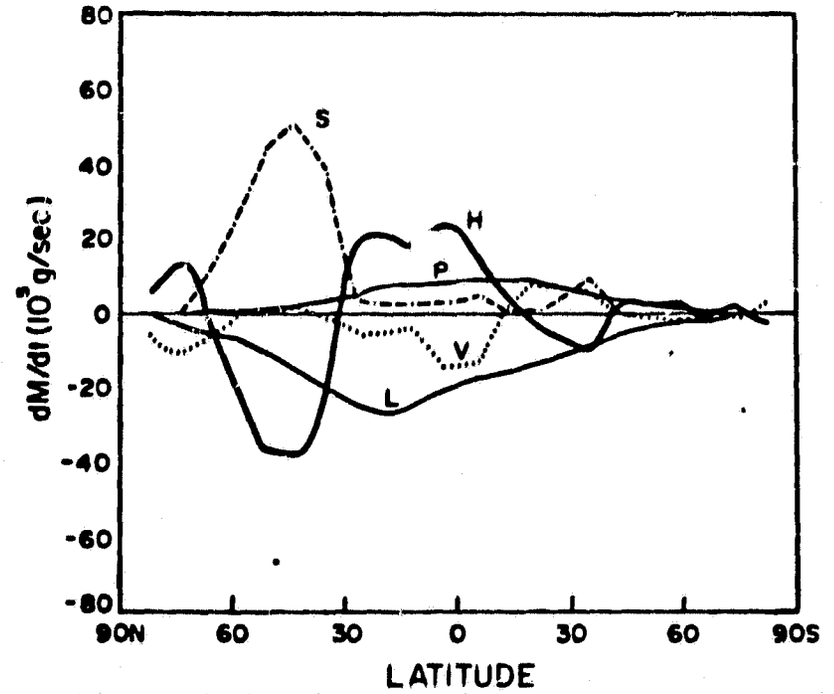

Figures 5a-b: Annual CO budget as a function of latitude. a) experiment T4, b) experiment T2. M - mass of tracer, H - horizontal flux covergence V - vertical transport inot the toposphere from the stratosphere, P and L - photochemical production and loss terms and S - the gonchemical surface source terms. Units are 10^3 g/sec.

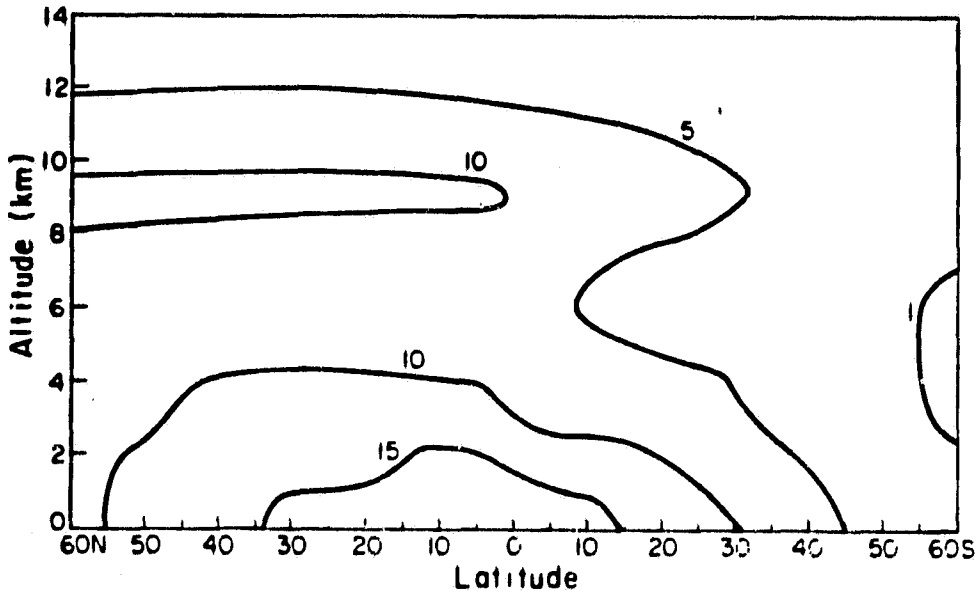

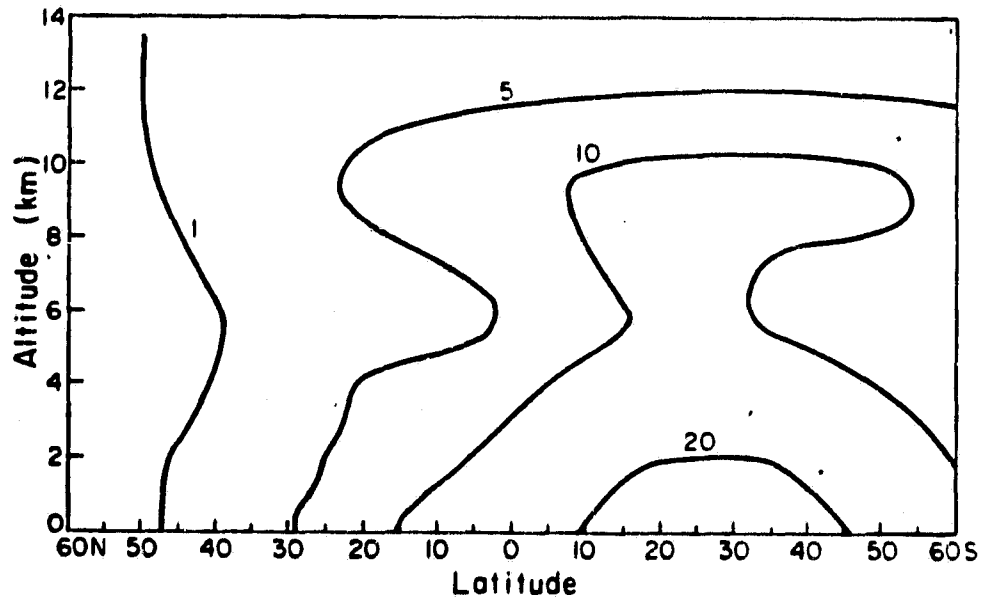

Figures 6a-b: Isopleths of the mean (diurnally averaged) OH concentrations in units of 10^5 molecules cm^{-3} in experiment T4. a) January, b) July.

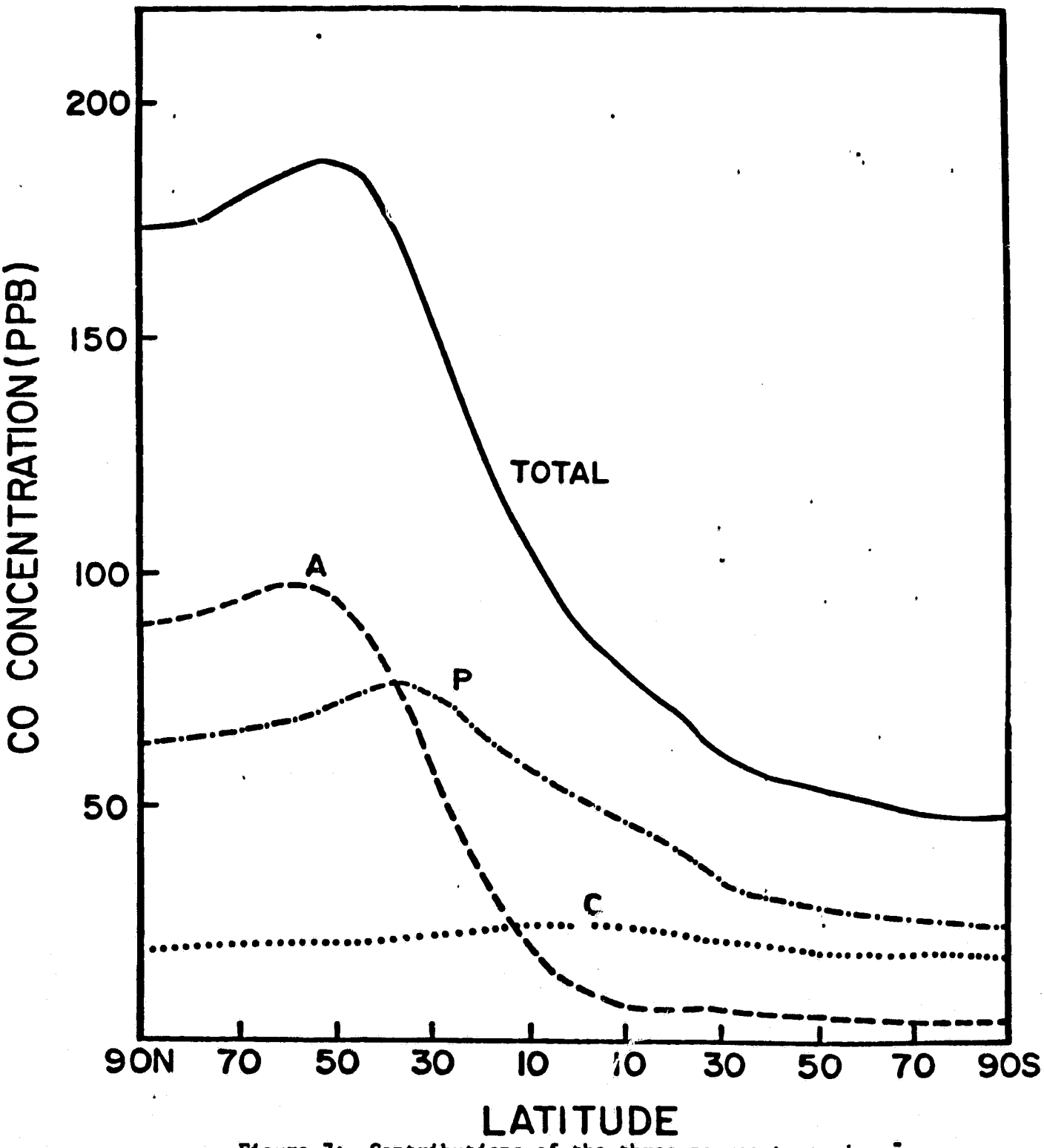

Figure 7: Contributions of the three source types in experiment T4. The curve labeled A refers to the anthropogenic component, P to the plant source and C to the source from methane oxidation.